

Differential cross sections and angular-correlation parameters for $n = 3$ excitations in hydrogen by electrons and positrons

A. K. Katiyar and Rajesh Srivastava

Department of Physics, University of Roorkee, Roorkee 247 667, India

(Received 25 April 1988; revised manuscript received 12 December 1988)

A distorted-wave Born approximation method has been used to calculate the differential cross sections and angular-correlation parameters for individual $1s \rightarrow 3l$ ($l=0,1,2$) transitions in hydrogen by electrons and positrons. The distortion in both the initial and final channels is incorporated due to static, polarization, and exchange effects. Calculated results are compared with the available other theoretical results.

INTRODUCTION

Most of the earlier work on electron-impact $n = 3$ excitations in hydrogen is theoretical. Different theories have been mainly applied to calculating total cross sections (TCS) for individual $1s \rightarrow 3l$ ($l=0, 1, \text{ and } 2$) transitions (see, for example, Srivastava and Rai,¹ Whelan *et al.*,² and Callaway *et al.*³). However, it is quite misleading to judge the success of a theoretical model purely on the agreement of the total cross sections with experimental measurements. In fact, differential cross sections (DCS) are known to provide better insight to a collisional process than the TCS and should also be calculated for the reliable assessment of a theoretical model. For $n = 3$ excitations in hydrogen, DCS results were reported by Tai *et al.*⁴ in the Glauber approximation (GA) for $1s \rightarrow 3s$ and $1s \rightarrow 3p$ excitations, at 100 eV incident-electron energy and in the limited range of scattering angles (up to 50°). In addition, Syms *et al.*,⁵ using distorted-wave polarized orbital (DWPO) theory and implementing distortion only in the initial channel, and van de Ree,⁶ using noniterative integral formalism (NIF), have reported the DCS for $1s \rightarrow 3l$ ($l=0, 1, \text{ and } 2$) excitations at the intermediate and low incident-electron energies, respectively.

An electron-photon angular-correlation experiment yields information about a scattering process which is far more detailed than the conventional scattering experiments and thus provides very sensitive tests for scattering theories.⁷⁻⁹ From the point of view of electron-photon correlation studies, excitation of the $n = 2$ states of hydrogen has received considerable attention both theoretically and experimentally.⁷⁻⁹ On the other hand, for $n = 3$ excitations in hydrogen not much attention has been paid,¹⁰⁻¹³ though such excitations are more interesting to study because of the involved greater multiplicities of the states. It is only recently that some results of the electron-photon coincidence rates for 3^2P_j and 3^2D_j states of hydrogen have been reported^{11,13} and there is further progress in the measurements of circular polarization results for these states.¹⁴

In this paper, we present our study of electron impact $n = 3$ excitations in hydrogen in a fairly more complete manner, especially with a view to understanding the an-

gular behavior of the scattering of these excitations. We adopt a reliable two-potential distorted-wave Born approximation (DWBA) to describe the excitation process and obtain results for DCS and angular-correlation parameters. In fact, the distorted-wave methods have become known in recent years as being rather simple and of wide applicability for the electron-atom excitation at intermediate energies.¹⁵⁻¹⁷

The interest in the positron-atom scattering has been stimulated by the intense positron-beam experiments.^{18,19} There is very close similarity between the electron and the positron collisions. The only difference between the two cases is that, in positron collisions, there is no process of electron exchange. Most of the theoretical methods adopted for electron collision can be easily extended to study similar positron collisions. Some calculations are already available for elastic and inelastic scattering of positrons from the hydrogen atom.^{16,20-23} Among these, our recent application¹⁶ of a DWBA to study $n = 2$ excitations in hydrogen has shown very interesting results. Except for the Coulomb-projected-Born (CPB) calculation²⁴ that results in giving the cross sections of $1s \rightarrow 3s$ excitation there is no other calculation available for positron-impact $n = 3$ excitations in hydrogen. These are therefore also considered in the present study.

THEORY

The T matrix is defined as¹⁵⁻¹⁷

$$T_{if} = \langle \Phi_f | V | \Psi_i^+ \rangle, \quad (1)$$

where Φ_f is the unperturbed wave function in the final channel, V is the interaction potential, and Ψ_i^+ is the exact wave function describing the system in the initial channel.

Now let \mathbf{r}_1 and \mathbf{r}_2 , respectively, be the position vectors of the bound electron of the target hydrogen and the projectile electron (positron) with respect to the hydrogen nucleus as origin. Then we can write

$$H\Psi = E\Psi \quad (2)$$

and

$$H_0\Phi = E\Phi, \quad (3)$$

where

$$E = \frac{1}{2}k_i^2 + \varepsilon_i = \frac{1}{2}k_f^2 + \varepsilon_f, \quad (4)$$

$$H_0 = -\frac{1}{2}\nabla_1^2 - \frac{1}{2}\nabla_2^2 - \frac{1}{r_1}, \quad (5)$$

and

$$H = H_0 + V \quad (6)$$

such that

$$V = Z' \left[\frac{1}{r_2} - \frac{1}{r_{12}} \right]. \quad (7)$$

$Z' = -1$ for electron and $+1$ for positron. \mathbf{k}_i and \mathbf{k}_f are the initial and final momentum vectors of the projectile electron (positron). ε_i and ε_f are initial and final eigenenergies of the target hydrogen atom.

On dividing the interaction potential V into two parts such as $V = U + W$ and using the two-potential formulation, we can write the T matrix in the following exact form:¹⁵⁻¹⁷

$$T_{if} = \langle \chi_f^- | U | \Phi_i \rangle + \langle \chi_f^- | W | \Psi_i^+ \rangle, \quad (8)$$

where χ satisfies in general the following equation:

$$(H_0 + U)\chi = E\chi. \quad (9)$$

The choice of U is arbitrary and in principle mathematically can be chosen anything so long as the relation $U = V - W$ is exactly satisfied. Our choice which

we shall mention later would be such that distortion of the projectile due to the static field of target and polarization of target is taken into account. However, we shall see that U is only a function of r_2 as it greatly simplifies the calculation¹⁵ and the first term in Eq. (8) drops out due to orthogonality of target wave functions. Therefore for an inelastic process we have

$$T_{if} = \langle \chi_f^- | W | \Psi_i^+ \rangle. \quad (10)$$

Since Ψ_i^+ , the exact solution of Eq. (2), is not possible to obtain,^{15,25} we adopt the following approximation for Ψ_i^+ which is obtained using the distorted-wave polarized orbital method as suggested and used by McDowell and his co-workers²⁶ as well as in our previous works:^{13,16}

$$\begin{aligned} \Psi_i^+ = & [\phi_i(\mathbf{r}_1) + \phi_{\text{pol}}(\mathbf{r}_1, \mathbf{r}_2)] F_s^+(\mathbf{k}_i, \mathbf{r}_2) \\ & + s \delta_{Z', -1} \phi_i(\mathbf{r}_2) F^+(\mathbf{k}_i, \mathbf{r}_1). \end{aligned} \quad (11)$$

Here $\phi_i(\mathbf{r}_1)$ is the unperturbed initial wave function of the target and $\phi_{\text{pol}}(\mathbf{r}_1, \mathbf{r}_2)$ represents its polarization term.¹⁶ s is $+1$ or -1 depending on the total spin of the scattering function in singlet or triplet mode. $F_s^+(\mathbf{k}_i, \mathbf{r}_2)$ is the outgoing distorted wave and is expanded as

$$F_s^+(\mathbf{k}_i, \mathbf{r}_2) = \sum_{l=0}^{\infty} \frac{2l+1}{\sqrt{k_i}} i^l e^{i\delta_l^s(k_i^2)} \frac{u_l^s(k_i, r_2)}{r_2} P_l(\hat{\mathbf{k}}_i \cdot \hat{\mathbf{r}}_2), \quad (12)$$

where δ_l^s is the phase shift of the l th partial wave and P_l is the Legendre polynomial of order l . Now we use this expression [Eq. (12)] in Eq. (11) which finally satisfies Eq. (2) to give the following integrodifferential equation:

$$\left[\frac{d^2}{dr^2} + k_i^2 - \frac{l(l+1)}{r^2} - 2V_{\text{stat}}(r) - 2V_{\text{pol}}(r) \right] u_l^s(k_i, r) = s \delta_{Z', -1} X_l^s(r) R_{1s}(r), \quad (13)$$

where $V_{\text{stat}}(r)$ and $V_{\text{pol}}(r)$ are, respectively, the static and polarization potentials having forms

$$V_{\text{stat}}(r) = \langle \phi_i | V | \phi_i \rangle = Z' \left[1 + \frac{1}{r} \right] e^{-2r}, \quad (14)$$

$$\begin{aligned} V_{\text{pol}}(r) = & -\frac{9}{4r^4} \left[1 - e^{-2r} (1 + 2r + 2r^2 + \frac{4}{3}r^3 + \frac{2}{3}r^4 \right. \\ & \left. + \frac{4}{37}r^5) \right]. \end{aligned} \quad (15)$$

The nonhomogeneous term $X_l^s(r)$ is due to electron exchange as given below:

$$\begin{aligned} X_l^s(r) = & (\varepsilon_{1s} - k_i^2) \delta_{l0} \int_0^{\infty} R_{1s}(t) u_l^s(k_i, t) t dt \\ & + \frac{2}{2l+1} \int_0^{\infty} R_{1s}(t) u_l^s(k_i, t) \frac{r_{<}^l}{r_{>}^{l+1}} dt. \end{aligned} \quad (16)$$

ε_{1s} is the eigenenergy of the ground $1s$ state of hydrogen. Further, Eq. (13) is to be solved with the usual following boundary conditions:

$$u_l^s(k_i, r) \sim 0 \quad r \rightarrow 0 \quad (17a)$$

and

$$u_l^s(k_i, r) \sim \frac{1}{\sqrt{k_i}} \sin \left[k_i r - \frac{l\pi}{2} + \delta_l^s \right] \quad r \rightarrow \infty \quad (17b)$$

We can write the following choice for χ_f^- :

$$\chi_f^-(\mathbf{r}_1, \mathbf{r}_2) = \phi_f(\mathbf{r}_1) \eta^-(\mathbf{k}_f, \mathbf{r}_2), \quad (18)$$

where $\phi_f(\mathbf{r}_1)$ is the final bound-state wave function of the hydrogen atom and $\eta^-(\mathbf{k}_f, \mathbf{r}_2)$ represents an ingoing distorted-wave function to be obtained from Eq. (9). For U we have the following choice as used previously with success by various authors^{17,27,28} which takes into account the distortion of the projectile by static and polarization potentials:

$$U(r) = V_{\text{stat}}(r) + V_{\text{pol}}(r). \quad (19)$$

With the use of this choice for U and using the following

expansion for $\eta^-(\mathbf{k}_f, \mathbf{r}_2)$:

$$\eta^-(\mathbf{k}_f, \mathbf{r}_2) = \frac{1}{\sqrt{k_f}} \sum_{l'=0}^{\infty} (2l'+1) i^{l'} e^{-i\delta_{l'}(k_f^2)} \frac{u_{l'}^-(k_f, r_2)}{r_2} P_{l'}(\hat{\mathbf{k}}_f \cdot \hat{\mathbf{r}}_2) \quad (20)$$

we see that $u_{l'}^-(k_f, r_2)$ satisfies

$$\left[\frac{d^2}{dr_2^2} + k_f^2 - \frac{l'(l'+1)}{r_2^2} - 2V_{\text{stat}}(r_2) - 2V_{\text{pol}}(r_2) \right] u_{l'}^-(k_f, r_2) = 0 \quad (21)$$

and has to be solved by using similar boundary conditions as given by Eq. (17).

Now we have defined $\chi_{\bar{f}}^-$ and $\Psi_{\bar{f}}^+$ in the expression [Eq. (10)] for T_{if} , which finally can be written as

$$T_{if}^s = T_{if}^{\text{dir}} + sT_{if}^{\text{ex}}, \quad (22)$$

where T_{if}^{dir} and T_{if}^{ex} are direct and exchange T matrices, respectively, given as

$$T_{if}^{\text{dir}} = \langle \eta^-(\mathbf{k}_f, \mathbf{r}_2) \phi_f(\mathbf{r}_1) | W | \phi_i(\mathbf{r}_1) F_s^+(\mathbf{k}_i, \mathbf{r}_2) \rangle \quad (23)$$

and

$$T_{if}^{\text{ex}} = \langle \eta^-(\mathbf{k}_f, \mathbf{r}_2) \phi_f(\mathbf{r}_1) | W | \phi_i(\mathbf{r}_2) F_s^+(\mathbf{k}_i, \mathbf{r}_1) \rangle \delta_{Z', -1}. \quad (24)$$

Following previous works^{16,17,29,30} and carrying out the straightforward but lengthy standard angular-momentum algebra as well as adopting the well-known Ochkur-Bonham approximation^{31,32} for the exchange T matrix (i.e., T_{if}^{ex}), we obtain the transition matrices for individual $1s \rightarrow 3l$ ($l=0,1,2$) excitations. The full details are, however, given elsewhere.³³ The radial Eq. (13) is solved for $u_l^-(k, r)$ by the noniterative procedure of Marriot.³⁴ In general, the normalization of $u_l(k, r)$ and phase shift are obtained by comparison with JWKB solution.³⁵

From the T matrices the differential cross sections for each transition in $1s \rightarrow 3l$ ($l=0,1,2$) excitations of hydrogen are evaluated in the conventional manner. The general way of writing the differential cross section is

$$\sigma_{1s \rightarrow 3lm}(\theta, \phi) = \frac{1}{4\pi^2} \frac{k_f}{k_i} \left[\frac{1}{4} |T_{1s \rightarrow 3lm}^+|^2 + \frac{3}{4} |T_{1s \rightarrow 3lm}^-|^2 \right], \quad (25)$$

with

$$T_{1s \rightarrow 3lm}^{\pm} = T_{1s \rightarrow 3lm}^{\text{dir}} \pm T_{1s \rightarrow 3lm}^{\text{ex}}. \quad (26)$$

Angular-correlation parameters

Information regarding the population of the magnetic substates can be obtained by measuring the angular correlation between the electron which excited the $3p$ (or $3d$) level and subsequently emitted photon. These measurements together with the differential cross sections completely define the scattering process.

For $1s \rightarrow 3p$ excitation

Similar to $1s \rightarrow 2p$ excitation in hydrogen for the case of $1s \rightarrow 3p$ excitation, the following are the angular correlation parameters:^{7,10,36-38}

$$\lambda = \frac{|f_{10}|^2}{|f_{10}|^2 + 2|f_{11}|^2} = \frac{\sigma_0(\theta, \phi)}{\sigma_0(\theta, \phi) + 2\sigma_1(\theta, \phi)}, \quad (27)$$

$$R = \frac{\text{Re}\langle f_{10}^* f_{11} \rangle}{\sigma(\theta, \phi)}, \quad (28)$$

$$I = \frac{\text{Im}\langle f_{10}^* f_{11} \rangle}{\sigma(\theta, \phi)}. \quad (29)$$

f_{10} and f_{11} are the excitation amplitudes for the $3pm$ magnetic sublevels with $m=0$ and 1 and can be obtained from the T matrix [Eq. (26)] in the usual manner. $\sigma_0(\theta, \phi)$ and $\sigma_1(\theta, \phi)$ are the corresponding differential cross sections. $\sigma(\theta, \phi) = \sigma_0(\theta, \phi) + 2\sigma_1(\theta, \phi)$ is the total differential cross section summed over the magnetic substate and $\langle \rangle$ denotes the spin-averaged value.

For $1s \rightarrow 3d$ excitation

Also of interest to us in the case of $1s \rightarrow 3d$ excitation are the following similar angular-correlation parameters:^{7,39}

$$\begin{aligned} \lambda_0(3d) &= \frac{|f_{20}|^2}{|f_{20}|^2 + 2|f_{21}|^2 + 2|f_{22}|^2} \\ &= \frac{\sigma_{20}(\theta, \phi)}{\sigma_{20}(\theta, \phi) + 2\sigma_{21}(\theta, \phi) + 2\sigma_{22}(\theta, \phi)}, \end{aligned} \quad (30)$$

$$\begin{aligned} \lambda_1(3d) &= \frac{2|f_{21}|^2}{|f_{20}|^2 + 2|f_{21}|^2 + 2|f_{22}|^2} \\ &= \frac{2\sigma_{21}(\theta, \phi)}{\sigma_{20}(\theta, \phi) + 2\sigma_{21}(\theta, \phi) + 2\sigma_{22}(\theta, \phi)}, \end{aligned} \quad (31)$$

as well as some relevant parameters obtainable through the real and imaginary parts of the bilinear combinations of the scattering amplitudes averaged over initial spins and summed over final spins, viz.,

$$\langle f_{20} f_{21}^* \rangle, \quad \langle f_{20} f_{22}^* \rangle, \quad \langle f_{21} f_{22}^* \rangle.$$

Here f_{2m} and $\sigma_{2m}(\theta, \phi)$ with $m=0,1,2$ are, respectively, the excitation amplitudes and differential cross sections for $3dm$ sublevel excitations which are related in the usual manner by the corresponding T matrices [Eq. (26)]. $\sigma = \sigma_{20}(\theta, \phi) + 2\sigma_{21}(\theta, \phi) + 2\sigma_{22}(\theta, \phi)$ is the total differential cross section summed over all magnetic substates.

However, $\langle f_{2m} f_{2m'}^* \rangle$ values do not directly define the quantities that are actually measured in a correlation experiment. As described by Andersen *et al.*³⁹ a set of four relative parameters would be adequate to describe a S - D excitation, the alignment angle γ , the angular momentum

L_1 , the linear polarization P_l , and density-matrix element ρ_{00} , which measures the relative height of the charge cloud. A correlation experiment may determine at the most three of these quantities, namely, γ , P_l , and ρ_{00} . In order to calculate these three parameters we use Eqs. (17a)–(17c) of the paper of Chwirot and Slevin¹² which define these three parameters in terms of the normalized multipole components $S_{2Q}(3D)$ of the reduced density matrix of the 3^2D_j state of hydrogen atoms. The $S_{2Q}(3D)$ values are obtained through the $\langle f_{2m} f_{2m'}^* \rangle$ quantities as described by us in our previous paper.¹³

RESULTS AND DISCUSSION

Since most of the other theoretical or experimental results for hydrogen are available at incident-electron energies (E_i) 54.4 and 100 eV we have also obtained our various results only at these energies. The DCS results for $1s \rightarrow 3l$ ($l=0, 1$, and 2) transitions and angular-

correlation parameters for $3p$ and $3d$ excited states in hydrogen are calculated, both by impact of electrons and positrons. All our results are displayed through Figs. 1–5 and Table I. In the different figures other theoretical results^{4–6,24,40} where available are included for comparison. First-order Born approximation (FBA) results are also calculated and compared in these figures.

Figures 1–3 show the DCS results, respectively, for $1s \rightarrow 3s$, $1s \rightarrow 3p$, and $1s \rightarrow 3d$ excitations. First, we discuss the comparison of our electron-impact DCS results with those obtained using FBA, GA,⁴ CPB,^{24,40} DWPO,⁵ and NIF (Ref. 6) methods. On comparison we find our DWBA results are in overall best agreement with the NIF results at 54.4 eV. At 100 eV our results compare favorably with the DWPO results. However, the difference between our DWBA results and the DWPO (Ref. 5) calculation is basically due to the inclusion of the distortion in the final channel in our model which was not considered in the DWPO method. As is well known,

TABLE I. Correlation parameters for $3p$ and $3d$ excited states of hydrogen by electron impact. The numbers in square brackets represent the power of 10 by which the preceding number is to be multiplied.

Energy (eV)	Angle (deg)	For $3p$ excitation		For $3d$ excitation		
		R	I	ρ_{00}	P_l	γ (deg)
54.5	0.0	2.12[−4]	−1.52[−6]	6.12[−1]	0.00	0.0
	5.0	3.19[−1]	−2.79[−2]	3.93[−1]	3.94[−2]	−31.0
	10.0	3.45[−1]	−5.55[−2]	3.98[−1]	1.87[−2]	−47.6
	15.0	3.11[−1]	−8.47[−2]	4.03[−1]	3.58[−2]	−54.9
	20.0	2.31[−1]	−1.19[−1]	4.06[−1]	3.97[−2]	−57.6
	25.0	2.55[−1]	−1.60[−1]	4.08[−1]	3.99[−2]	−57.8
	30.0	2.25[−1]	−2.07[−1]	4.08[−1]	3.74[−2]	−56.2
	40.0	1.25[−1]	−2.69[−1]	3.91[−1]	2.35[−2]	−49.8
	50.0	1.59[−2]	−1.62[−1]	3.63[−1]	1.20[−2]	−43.4
	60.0	−2.63[−2]	1.35[−2]	3.52[−1]	2.01[−2]	−39.9
	70.0	−3.92[−2]	1.32[−1]	3.70[−1]	2.50[−2]	−38.2
	80.0	−3.58[−2]	2.11[−1]	4.13[−1]	3.09[−2]	−36.0
	100.0	1.61[−2]	2.49[−1]	4.64[−1]	2.52[−2]	−12.5
	120.0	7.99[−2]	2.21[−1]	4.22[−1]	2.22[−2]	6.1
	140.0	1.07[−1]	1.55[−1]	4.23[−1]	2.57[−2]	5.5
	160.0	7.42[−2]	7.20[−2]	4.04[−1]	2.03[−2]	3.1
	180.0	0.00	0.0	3.88[−1]	1.06[−5]	0.0
	100.0	0.0	6.41[−4]	−2.12[−5]	6.12[−1]	0.00
5.0		3.45[−1]	−2.63[−2]	3.95[−1]	2.57[−2]	−50.0
10.0		2.69[−1]	−5.24[−2]	4.01[−1]	4.37[−2]	−63.7
15.0		2.31[−1]	−8.15[−2]	4.06[−1]	4.51[−2]	−67.2
20.0		2.13[−1]	−1.22[−1]	4.14[−1]	4.54[−2]	−66.9
25.0		1.98[−1]	−1.84[−1]	4.22[−1]	4.42[−2]	−63.5
30.0		1.77[−1]	−2.56[−1]	4.23[−1]	3.68[−2]	−56.9
40.0		1.18[−1]	−2.17[−1]	3.86[−1]	2.18[−2]	−40.1
50.0		6.20[−2]	6.39[−2]	3.62[−1]	3.11[−2]	−33.2
60.0		8.90[−2]	1.36[−1]	3.83[−1]	3.48[−2]	−32.4
70.0		7.48[−2]	2.70[−1]	4.27[−1]	3.73[−2]	−32.9
80.0		8.71[−2]	2.31[−1]	4.92[−1]	3.49[−2]	−31.0
100.0		9.93[−2]	2.36[−1]	5.06[−1]	1.52[−2]	5.9
120.0		9.78[−2]	2.05[−1]	4.43[−1]	3.59[−2]	16.7
140.0		6.04[−2]	1.47[−1]	4.28[−1]	3.88[−2]	13.5
160.0		4.46[−2]	7.48[−2]	4.09[−1]	2.90[−2]	6.2
180.0		0.00	0.00	3.88[−1]	1.56[−5]	0.0

GA and FBA results compare well with our DWBA results only in smaller scattering angles while failing to follow our results at larger scattering angles. The CPB results⁴⁰ for $1s \rightarrow 3s$ excitation are also in good agreement with our results at 100 eV.

Further, from Figs. 1–3, when we compare our electron- and positron-impact results for each transition (i.e., $1s \rightarrow 3s$, $3p$, or $3d$), we find that they do not differ much at 100 eV. However, they differ slightly for larger scattering angles at 54.4 eV. The difference in the electron- and positron-impact results at lower incident energies and for larger scattering angles is quite expected and is mainly due to the dominant contribution of electron exchange and polarization distortion effect at such energies.

Our calculated λ values for $3p$ excitation in hydrogen

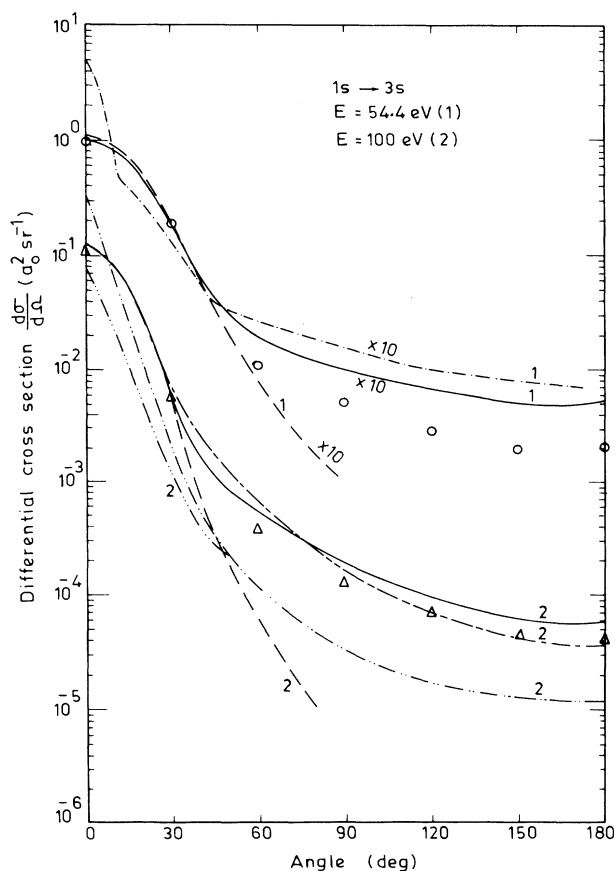


FIG. 1. Differential cross sections for the $1s \rightarrow 3s$ transition of hydrogen at electron-impact energies 54.4 and 100 eV. The curves numbered 1 and 2 are, respectively, at 54.4 and 100 eV. The positron results are shown by circles and triangles, respectively, at 54.4 and 100 eV. —, present DWBA results. - - -, close-coupling results of van de Ree (Ref. 6). — · — · —, DWPO results of Syms *et al.* (Ref. 5). ·····, Coulomb projected Born results of Saxena (Ref. 40). — · — · —, Glauber results of Tai *et al.* (Ref. 4). - - -, first-order Born results.

are plotted against angle of scattering (θ) in Fig. 4. At 100 eV of incident-electron energy, present results are compared with the GA (Ref. 10) results as well as with the FBA results. First we compare our electron-impact results at two different energies. Since λ denotes the relative contribution of the differential cross section from the $m=0$ sublevel excitation of the $3p$ state to the total DCS for $3p$ excitation, we find from Fig. 4 that in our results for scattering through $\theta < 25^\circ$ and $\theta > 65^\circ$, the excitation of the $m = \pm 1$ sublevels dominates with increasing incident-electron energy, except near the forward ($\theta = 0$) and backward ($\theta = \pi$) angles when only $m = 0$ sublevel excitation occurs. As we know the total cross section is dominated by the contribution of the DCS coming from near forward scattering angles, therefore, we can say that in the case of $3p$ excitation the total cross sections at high energies are primarily controlled by $m = \pm 1$ sublevel excitations. The comparison of our electron-impact results at 100 eV with the available GA results up to 50° and FBA results suggests that GA and FBA are not much different from each other but differ considerably with ours at higher scattering angles ($\theta > 10^\circ$). This feature is quite expected as GA or FBA gives DCS results which differ at intermediate and backward scattering angles with distorted-wave calculations because of the absence

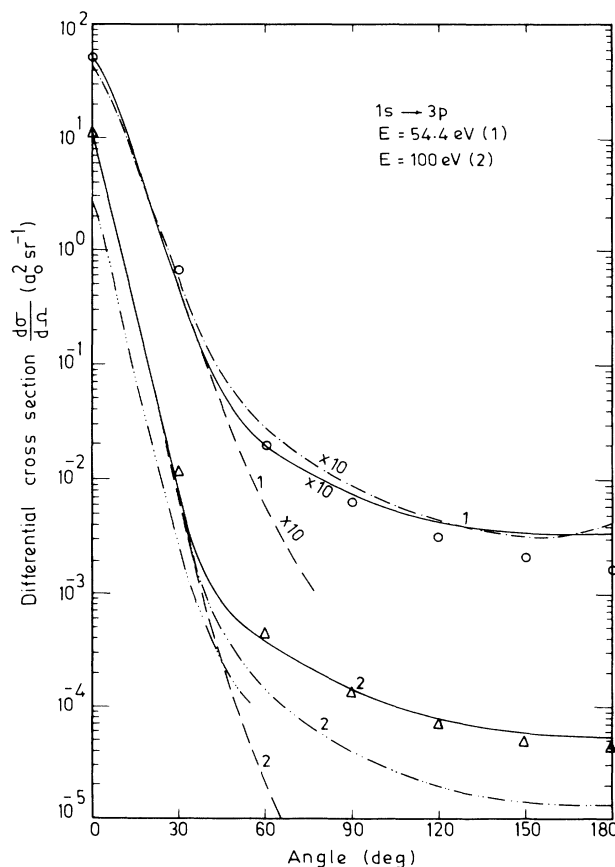


FIG. 2. Same as Fig. 1 but for the $1s \rightarrow 3p$ transition in hydrogen.

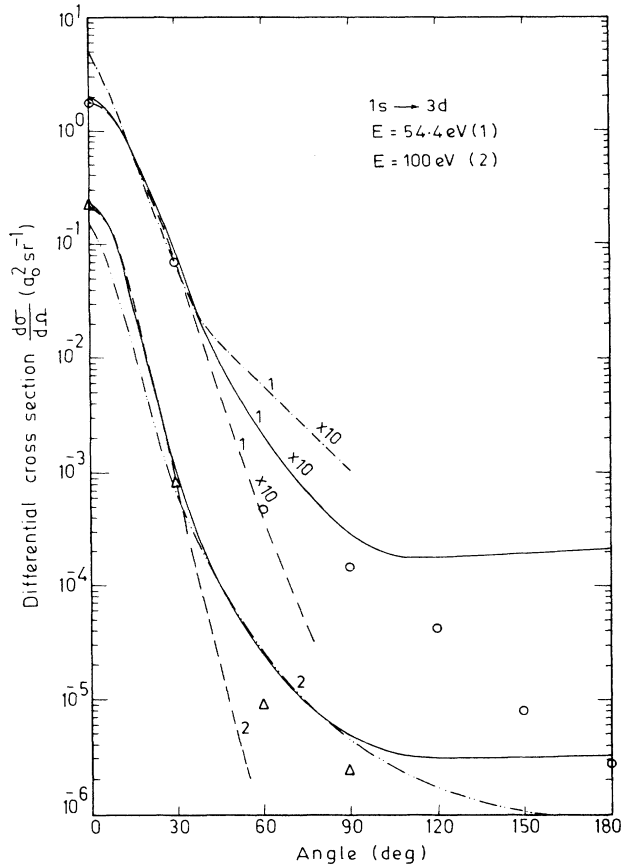


FIG. 3. Same as Fig. 1 but for the $1s \rightarrow 3d$ transition in hydrogen.

of appropriate distortions of the incident electron in their formulation. When we compare our positron-impact results at two different energies we find that the comparison is similar to that as in the case of electron impact. Fur-

ther comparison of λ values for the electron-impact case to the corresponding positron suggests that the positron-impact λ curves are having much deeper and broader minima than the electron impact. Consequently, we can say, for $3p$ excitation by positrons, the $m = \pm 1$ sublevels contribute more to total cross sections as compared to impact of similar energy electrons.

Similar to Fig. 4, Figs. 5(a) and 5(b), respectively, show our results of λ_0 and λ_1 for $3d$ excitation in hydrogen as defined by Eqs. (30) and (31). First, we compare in Fig. 5(a) our results for λ_0 which is the relative contribution of the DCS for the $m = 0$ sublevel of the $3d$ state to its total DCS having contributions from $m = 0, \pm 1$, and ± 2 sublevels of the $3d$ state. The behavior of λ_0 with respect to scattering angles and incident projectile energies is quite similar to that presented in Fig. 4 for λ in the case of $3p$ excitation. However, for λ_0 in the case of $3d$ excitation, the first minimum at each energy extends roughly in the wider range of scattering angles and is having relatively much lower values of λ_0 . From Fig. 5(b), which shows results for λ_1 (i.e., relative contribution of DCS from $m = \pm 1$ substates to total DCS), we find that the λ_1 curves have almost reverse behavior to that of λ_0 curves as displayed in Fig. 5(a). If we remember that $1 - \lambda_0 - \lambda_1$ represents the relative contribution of the excitation of $m = \pm 2$ substates to the total DCS then we can easily assess from Figs. 5(a) and 5(b) the individual contribution of the excitation of each substate of the $3d$ excited state. By careful comparisons of λ_0 and λ_1 curves and following the discussions as presented for Fig. 4 we can easily show that the total cross section for $3d$ state excitation is dominated by its $m = \pm 1$ and ± 2 substate components. The effect of increasing the incident-electron energy on total cross section is to have more contribution from $m = \pm 2$ substates to it followed by the contributions of $m = \pm 1$ and 0 substates.

Further intercomparison of our electron and positron results [in Figs. 5(a) and 5(b)] at each incident projectile

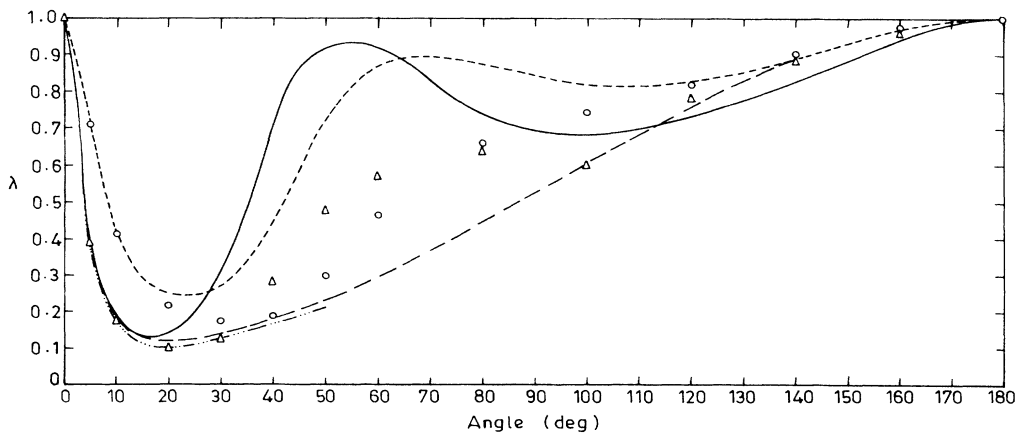


FIG. 4. λ parameters for the $3p$ state of hydrogen by electron and positron impact. —, present DWBA results at $E_i = 100$ eV (electron). ----, present DWBA results at $E_i = 54.4$ eV (electron). - · - · -, Glauber results of Chan and Chang (Ref. 10). Δ , present DWBA results at $E_i = 100$ eV (positron). \circ , present DWBA results at $E_i = 54.4$ eV (positron). - - -, first-order Born results.

energy as well as mutual comparison of positron results at two different energies suggest that positron-impact λ_0 and λ_1 results show large variations in the results with the increase of incident energy as compared to electron-impact results and also favor more the excitation of $m = \pm 2$ substates as the positron-impact energy is increased. Finally, the Glauber results¹⁰ when compared with our results are found to give λ_0 and λ_1 values somewhat different in magnitude than ours but showing similar shape and nature. FBA results, as well known, fail to reproduce our results at larger scattering angles except below 10° of scattering angles.

In our previous paper¹³ using our present calculation of the scattering amplitudes for $3p$ and $3d$ excited states at $E_i = 54.4$ and 100 eV for scattering angles of 20° and 25° we reported electron-photon coincidence rates which showed very good agreement with the experimental results of Chwirot and Slevin.¹² Since there are no other results available for further comparison with our R and I correlation parameters for 3^2P excitation, we simply compile our electron-impact results for these parameters in Table I. However, the behavior of our R and I results with respect to scattering angle is of a similar nature as one sees for 2^2P excitation in hydrogen.⁹

In Table I we have also displayed our electron-impact

results for γ , P_l , and ρ_{00} parameters for 3^2D excitation. We find our results for the alignment angle γ of the charge cloud varies with scattering angle such that first a deep negative minimum occurs and then it shows a positive maximum before becoming zero at 180° of scattering angle. While the linear polarization P_l and ρ_{00} which measure relative height of the charge cloud vary in oscillating manner with respect to scattering angle but there is not much variation in their magnitudes. However, for 3^2D excitation, results for γ , P_l , and ρ_{00} parameters are also obtained for only two scattering angles, viz., 20° and 25° by Chwirot and Slevin¹² which they derived from their electron-photon coincidence rate measurements, but their results differ significantly from ours and do not provide any meaningful comparison. Until more measured data are available it would be premature to comment about these parameters. We have also obtained first-order Born results for the three parameters by setting in our DWBA code the distortion potential and exchange contribution to be zero. Our so obtained first-order Born results for the alignment angle γ are found to match exactly with the first-order Born results tabulated by Andersen *et al.*³⁹ at 54.5 and 100 eV of energies for 20° and 25° of scattering angles. Although we do not present here comparison of our DWBA and FBA results for the three

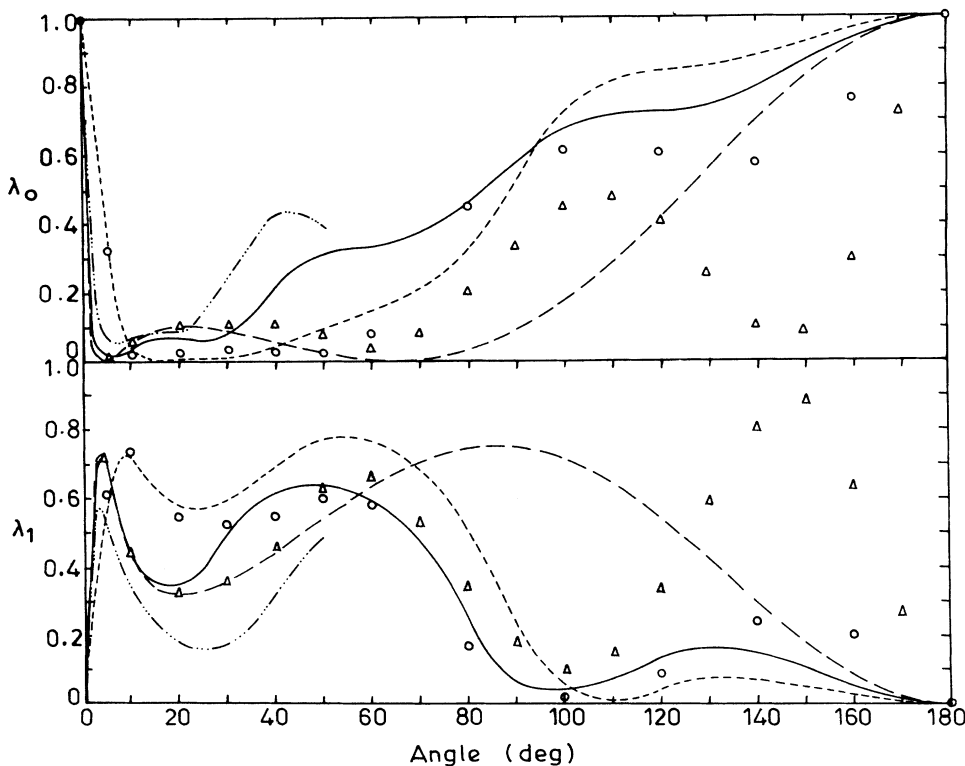


FIG. 5. (a) λ_0 parameters for the $3d$ state of hydrogen by electron and positron impact. The description of the curves is the same as in Fig. 4. (b) λ_1 parameters for the $3d$ state of hydrogen by electron and positron impact. The description of the curves is the same as in Fig. 4.

parameters, we wish to mention that both the results compare in the usual expected manner, i.e., DWBA results differ with FBA more at lower energies and at intermediate and backward scattering angles. We hope all our results presented in Table I will be useful for future comparison purposes.

Finally, we wish to add that our use of the Ochkur-Bonham approximation (OBA) to evaluate the exchange T matrix (for electron excitation) in the present DWBA calculation may raise some doubts as to the reliability of our results. In fact, justification of the use of OBA has been discussed in many earlier papers⁴¹ and reviews.^{25,42} Also, some reliable calculations⁴³⁻⁴⁵ have used this approximation recently. However, in our present paper, since the results reported are at 54.4 and 100 eV (which are nearly more than four times the threshold excitation energies of $n=3$ excitations) we strictly believe that whatever approximation is adopted to evaluate the ex-

change T matrix at such energies would give the same contribution for exchange as obtained through OBA. To have an idea about the error which may get introduced by the use of OBA we repeated the calculation of Shelton *et al.*⁴⁶ for $1s \rightarrow 2s$ excitation in hydrogen but using the OBA for evaluation of their exchange T matrix. We found our so calculated results for DCS at 54.4 eV differed with their⁴⁶ reported results within only 7%. Similar uncertainty in our present electron-impact results for $n=3$ excitations may also be expected by the use of OBA.

ACKNOWLEDGMENTS

One of us (A.K.K.) is thankful to the Council of Scientific and Industrial Research (CSIR), India, for financial assistance.

- ¹R. Srivastava and D. K. Rai, *J. Phys. B* **11**, 309 (1978).
²C. T. Whelan, M. R. C. McDowell, and P. W. Edmunds, *J. Phys. B* **20**, 1587 (1978).
³J. Callaway, K. Unnikrishnan, and D. H. Oza, *Proceedings of the Fifteenth International Conference on the Physics of Electronic and Atomic Collisions, Brighton, United Kingdom, 1987*, edited by J. Geddes, H. B. Gilbody, A. E. Kingston, C. J. Latimer, and H. R. J. Walters (Queen's University, Belfast, 1987).
⁴H. Tai, R. H. Bassel, E. Gerjuoy, and V. Franco, *Phys. Rev. A* **1**, 1919 (1970).
⁵R. F. Syms, M. R. C. McDowell, L. A. Morgan, and V. P. Myerscough, *J. Phys. B* **8**, 2817 (1975).
⁶J. van de Ree, *J. Phys. B* **15**, 2245 (1982).
⁷K. Blum and H. Kleinpoppen, *Phys. Rep.* **52**, 203 (1979).
⁸G. F. Hanne, *Phys. Rep.* **95**, 95 (1983).
⁹J. Slevin, *Rep. Prog. Phys.* **47**, 461 (1984).
¹⁰F. T. Chan and C. H. Chang, *Phys. Rev. A* **15**, 118 (1977).
¹¹S. Chwirot and J. Slevin, *J. Phys. B* **20**, 6139 (1987).
¹²S. Chwirot and J. Slevin, *J. Phys. B* **20**, 3885 (1987).
¹³A. K. Katiyar and R. Srivastava, *J. Phys. B* **20**, L821 (1987).
¹⁴J. Slevin (private communication).
¹⁵Y. Itikawa, *Phys. Rep.* **143**, 69 (1986).
¹⁶R. Srivastava, A. K. Katiyar, and I. Khurana, *J. Phys. B* **20**, 1853 (1987).
¹⁷R. Srivastava, M. Kumar, and A. N. Tripathi, *J. Chem. Phys.* **82**, 1818 (1985); A. K. Katiyar and R. Srivastava, *Phys. Rev.* **38**, 2767 (1988).
¹⁸L. M. Diana, L. S. Fornari, S. C. Sharma, P. K. Pendleton, and P. G. Coleman, in *Positron Annihilation*, Proceedings of the Seventh International Conference on Positron Annihilation, New Delhi, India, 1985, edited by P. C. Jain, R. M. Singru, and K. P. Gopinathan (World Scientific, Singapore, 1985), p. 342.
¹⁹T. S. Stein and W. E. Kaupilla, in *Electronic and Atomic Collisions, Invited Papers of the XIV International Conference on the Physics of Electronic and Atomic Collisions, Palo Alto, 1985*, edited by D. C. Lorentz, W. E. Meyerhof, and J. R. Peterson (Elsevier Science, New York, 1986), p. 105.
²⁰R. J. Drachman and A. Temkin, *Case Studies in Atomic Collision Physics* (North-Holland, Amsterdam, 1972), Vol. 2, p. 399.
²¹A. S. Ghosh, N. C. Sil, and P. Mandal, *Phys. Rep.* **87C**, 313 (1982).
²²T. C. Griffith and G. R. Heyland, *Phys. Rep.* **39C**, 170 (1978).
²³T. S. Stein and W. E. Kaupilla, *Adv. At. Mol. Phys.* **10**, 53 (1983).
²⁴S. Saxena, G. P. Gupta, and K. C. Mathur, *J. Phys. B* **17**, 3743 (1984).
²⁵J. Callaway, *Adv. Phys.* **29**, 771 (1980).
²⁶T. Scott and M. R. C. McDowell, *J. Phys. B* **8**, 1851 (1975); **9**, 2235 (1976).
²⁷D. H. Madison, *J. Phys. B* **12**, 3399 (1979).
²⁸M. Stewart and D. H. Madison, *Phys. Rev. A* **23**, 647 (1981).
²⁹M. R. C. McDowell, L. A. Morgan, and V. P. Myerscough, *J. Phys. B* **6**, 1435 (1973).
³⁰K. L. Baluja, M. R. C. McDowell, L. A. Morgan, and V. P. Myerscough, *J. Phys. B* **11**, 715 (1978).
³¹V. I. Ochkur, *Zh. Eksp. Teor. Fiz.* **45**, 734 (1963) [*Sov. Phys.—JETP* **18**, 503 (1964)].
³²R. A. Bonham, *J. Chem. Phys.* **36**, 3260 (1962).
³³A. K. Katiyar, Ph.D. thesis, University of Roorkee, Roorkee, India, 1988.
³⁴R. Marriot, *Proc. Phys. Soc.* **72**, 121 (1958).
³⁵A. Burgess, *Proc. Phys. Soc.* **81**, 442 (1963).
³⁶U. Fano and J. H. Macek, *Rev. Mod. Phys.* **45**, 553 (1973).
³⁷A. E. Kingston, Y. C. Liew, and P. G. Burke, *J. Phys. B* **15**, 2755 (1982).
³⁸L. A. Morgan and M. R. C. McDowell, *J. Phys. B* **8**, 1073 (1975).
³⁹N. Andersen, J. W. Gallagher, and I. V. Hertel, *Phys. Rep.* **165**, 1 (1988).
⁴⁰S. Saxena, Ph.D. thesis, University of Roorkee, Roorkee, India, 1984.
⁴¹F. W. Byron, Jr. and L. J. Latour, *Phys. Rev. A* **13**, 649 (1976).
⁴²H. R. J. Walters, *Phys. Rep.* **116**, 1 (1984).
⁴³M. A. Dillon and M. Inokuti, *J. Chem. Phys.* **76**, 5887 (1982).
⁴⁴M. R. C. McDowell, P. W. Edmunds, R. M. Potvliege, C. J. Joachain, R. Singhal, and B. H. Bransden, *J. Phys. B* **17**, 3951 (1984).
⁴⁵S. Saxena and K. C. Mathur, *J. Phys. B* **18**, 509 (1985).
⁴⁶W. N. Shelton, E. S. Leherissey, and D. H. Madison, *Phys. Rev. A* **3**, 242 (1971).